Magnetic Structure of Force-Free Currents

Donald E. Scott

Abstract — **The fundamental vector calculus definition of a force-free, field-aligned current in space is expanded in cylindrical coordinates to obtain the partial differential equations that specify the magnetic field created by such a current. The primary resulting equation is identified as a Bessel equation of order zero in the variable *r*, the radial distance from the current axis. The Bessel function of the first kind and zeroth order is the solution for the axial (collinear) component of the field in closed form. The additional resulting equation for the angular (linking or azimuthal) component of the field is solved by the Bessel function of the first kind and first order. The equations also are put into state-variable form and an Euler step-wise approximation incorporating a 4th order Runge-Kutta algorithm is applied and this solution confirms the closed form results for both the linking and collinear components of the force-free magnetic field. The results show that (1) both of these magnetic components cyclically reverse their directions and vary in magnitude with increasing radial distance from the central axis of the current. (2) the magnetic field extends relatively farther from the central axis of a force-free current than it would from a current in a long straight wire--the total field magnitude varies inversely as the square root of *r* for large *r*. These results are shown to be consistent with laboratory and astronomical observations.**

Index Terms—**Plasma physics, Birkeland currents, flux-ropes, plasma, magnetic confinement, plasma sheaths, minimum-energy fields, Lorentz force, field-aligned currents, counter-rotating currents, diocotron instabilities.**

I. Introduction

SOME INVESTIGATORS, using mathematical models based on the premise that gravity is the dominant force in the universe, have expressed the opinion that gravity-based theory suggests that electromagnetic (EM) forces associated with current flow in space may be present, but have little or no substantive effect. In contrast to this judgment, there is a growing field that may be called "plasma-astrophysics". Its birth occurred in the opening years of the 20th century.

The "Northern Lights" (aurora Borealis and aurora Australis) remained mysterious phenomena for centuries. The answer to the question of what they are and how they are powered was provided by Kristian Birkeland (1867-1917) who made on-site electrical and geomagnetic measurements of those displays in northern Norway.

He suggested[1] the auroras were powered by "corpuscular rays" emanating from the Sun that become deflected into Earth's Polar Regions by the geomagnetic field. The existence of such magnetic field-aligned currents was strongly disputed based partially on the idea that currents could not cross the vacuum of space[2]. Birkeland's main problem was that although he had made detailed measurements of Earth's geomagnetic field on the ground and then wanted to extrapolate that information into a description of the current-density distribution that caused those magnetic effects, this is not possible. But time was on his side.

In 1962, instruments on NASA's Mariner II[3] space probe directly recorded the existence of plasma (called ionized gas at that time) coming from the Sun, and in 1966 a U.S. Navy navigation satellite[4], 1963-38C, observed at an altitude ~1100 km, anomalous magnetic behavior on nearly every pass over Earth's Polar Regions. Birkeland had suggested that such magnetic perturbations (now called "sub-storms") are caused by currents which stream from the Sun and flow almost vertically downward parallel to the geomagnetic field's direction. But he had no proof until those satellites flew – many years after his death.

Those vertical currents were first called Birkeland currents in 1967 by Alex Dessler[5]. Falthammer[6] (1986) states: "A reason why Birkeland currents are particularly interesting is that, in the plasma forced to carry them, they cause a number of plasma physical processes to occur (wave instabilities, fine structure formation)." NASA and its scientists have been working on Birkeland currents and "flux rope" observations since the mid-to-late-70's, with substantial activity on this topic after the late 80's. In 1995 T. Potemra[7] concluded that "Birkeland currents and Alfvén waves are fundamental to an understanding of the Earth's plasma environment." In 2009 space probe Themis discovered a flux rope[8] pumping a 650,000 A current down into the Arctic.

II. Definition of a Field-Aligned Current

Space plasmas consist of ionized and un-ionized gas, and dust. Consider a stream of moving charged particles (an electrical current) in such a plasma that is not subjected to any externally applied forces such as externally imposed electric or magnetic fields. A useful mathematical idealization of a physical cosmic current is a vector field of current density, ***j***, that, when viewed in a cylindrical coordinate system, creates an overall average current

Donald E. Scott, retired, was with the Electrical Engineering Department, University of Massachusetts/Amherst, MA 01002 for 39 years. He resides in Scottsdale, AZ 85262. (email dascott3@cox.net). The work described in the paper was not supported by any funding agency. All unreferenced work presented is the author's own work or is in the public domain.

vector, ***I***, which, by definition determines the direction of the z-axis. The magnitude of ***I*** is assumed to be everywhere independent of the *z* coordinate.

The electromagnetic force that is experienced by each charge within the plasma is given by

$$\boldsymbol{F} = q(\boldsymbol{E} + \boldsymbol{v} \times \boldsymbol{B}) \tag{1}$$

where the first term, $q\boldsymbol{E}$, is properly called the *electric force* and the second term, $q(\boldsymbol{v} \times \boldsymbol{B})$, is called the *magnetic force*. The name 'Lorentz force' is now often used to describe the entire expression (1).

The driving source of the total current, ***I***, within the plasma is not hypothesized here, but one example suggested by observations is that ***E*** in expression (1) could be the result of an induction process – current set in motion by the relative motion between a magnetic field and the conducting plasma possibly at an extreme distance from the site of our analysis. The plasma region contains the current stream, and this region is assumed to be cylindrical. Its radius is not assumed to be known at the outset. Nor are any assumptions made about the distribution of the current density across the cross-section. The plasma is limited in size by some maximum radius value *R* such that the analysis offered here is valid only within a range $0 < r < R$.

Even assuming this current is free of externally applied forces, any flow of charge creates its own magnetic field through which the charge flows. Each charged particle, *q*, in the stream is the origin point of two local vectors: $\boldsymbol{j} = q\boldsymbol{v}$ (current density) and ***B*** (magnetic field). The current density vector ***j*** at each point inherently creates a curl(***B***) vector given by one of Maxwell's equations

$$\nabla \times \boldsymbol{B} = \mu\left(\boldsymbol{j} + \varepsilon \frac{\partial \boldsymbol{E}}{\partial t} \right). \tag{2}$$

The derivative term in (2) which was added by Maxwell is called the *displacement current*. It is often considered to be zero valued, as we do here, when it can be assumed there are no time-varying electric fields in the region.

Integrating the curl(***B***) vectors over a cross-section of the stream (Stoke's theorem) yields

$$\int_S \nabla \times \boldsymbol{B} \bullet d\boldsymbol{S} = \int_S \mu \boldsymbol{j} \bullet d\boldsymbol{S} = \oint_C \boldsymbol{B} \bullet d\boldsymbol{l} \tag{3}$$

where *S* is any cross-sectional area of the (assumed cylindrical) plasma, and μ and ε are the permeability and permittivity respectively of the plasma medium. The result of (3) is the magnetic density, ***B***. Expression (2) is the *point form* and (3) is the *integral form* of that Maxwell equation.

It is important to realize that expression (2) is valid at any point. Explicitly, the current density vector, ***j***, at that point creates a curl(***B***) vector, not the local ***B*** vector itself. The integral form shown in (3) implies that ***B*** is a vector sum of the effects of all the ***j*** vectors on surface ***S*** which is enclosed by *C*.

The quantity called the *magnetic intensity* (symbol ***H***) is often used to describe the forcing function that creates the magnetic field, ***B***.

$$H = \frac{B}{\mu} = \frac{NI}{l} \tag{4}$$

H's dimensions are A/m (The number of turns, *N*, is dimensionless). *H* has also been variously called the *magnetizing field strength*, and the *magnetizing force*.

B in (4) arises from the integral form (3). In (4), ***B*** is clearly shown to be the result of ***I***, not any single ***j***. In (2) it should be clear that ***j*** creates a curl(***B***) vector, not a ***B*** vector. In general, there may well be (and often is) a non-zero valued ***B*** vector at a point at which $\boldsymbol{j} = 0$.

It may be shown that the energy density (*Joules/m*^{3}) stored in the magnetic field of such a current stream is given by

$$W_B = \frac{B^2}{2\mu} = \frac{\mu}{2} H^2 \tag{5}$$

which shows that the only way to reduce the entire stored energy to zero is to cut off the current (set $\boldsymbol{I} = 0$). In which case the entire cosmic current structure would cease to exist.

The dimensions of the involved quantities are:

$$\mu = \frac{B}{H} = \frac{Webers}{m^2} \frac{m}{A} = \frac{Webers}{mA} \tag{6}$$

$$\nabla \times B = \mu j = \frac{Webers}{mA} \frac{A}{m^2} = \frac{Webers}{m^3} \tag{7}$$

Prior to the time a cosmic current system, free of externally applied forces or fields, reaches a steady-state configuration, the ***j*** and ***B*** vectors are interacting – all the ***j***s are creating curl(***B***) vectors that sum to form the local ***B*** vectors. A force-creating interaction unavoidably exists everywhere between each non-zero valued current density vector and its local magnetic field vector. This force is a magnetic *Lorentz force* vector and is given by the second term in (1).

The vector cross product of a moving charge's velocity vector ***v*** and the local magnetic field vector ***B*** implies that the scalar value (magnitude) of the resulting force on each *q* is given by

$$F_L = qvB\sin\varphi \tag{8}$$

where φ is the smallest angle between the vectors $\boldsymbol{v}$ and $\boldsymbol{B}$, with scalar values v and B. We call φ the *Lorentz angle*. If this angle is zero or 180 degrees, the magnetic Lorentz $\boldsymbol{v} \times \boldsymbol{B}$ force at that point is zero-valued.

It is assumed that in an unconstrained space plasma, the current is free to move and distribute itself so as to minimize the internally stored potential energy due to the stress resulting from magnetic Lorentz forces everywhere throughout the plasma. In fact space plasmas are uniquely situated to obey the *minimum total potential energy principle*[9] which asserts that a structure or body shall deform or displace to a position and/or morphology that minimizes its total potential (stored) energy.

The electric current-density within a cosmic plasma (and the magnetic field it creates) are, consistent with the minimum total potential energy principle, free to seek a steady-state configuration in which the energy stored in its Lorentz forces is a minimum. The energy described in (5), however, is irreducible because it is caused by the fixed quantity, $\boldsymbol{I}$. But the Lorentz energy can be eliminated because it does not depend on the value of $\boldsymbol{I}$, only on the cross-products between local $\boldsymbol{B}$ and $\boldsymbol{j}$ vectors.

The process of shedding the internal magnetic-force energy may take an extended time to reach a steady-state equilibrium, but if and when it does, this arrangement is called a *force-free current* and is defined by the relation between the magnetic field vector, $\boldsymbol{B}$, and the current density vector $\boldsymbol{j}$, at every location at which a charge, q, is located in the current stream.

$$0 = \boldsymbol{F} = q\left(\boldsymbol{v} \times \boldsymbol{B}\right) = \boldsymbol{j} \times \boldsymbol{B} \tag{9}$$

With v ≠ 0 and B ≠ 0 it follows from (9) the Lorentz forces are everywhere = 0. Every $\boldsymbol{j}$ is collinear with its corresponding $\boldsymbol{B}$. This arrangement is therefore also called a *field-aligned current*.

It follows directly from (2) and (9) that, if there is no time-varying electric field present, then (9) is equivalent to

$$\left(\nabla \times \boldsymbol{B}\right) \times \boldsymbol{B} = 0 \tag{10}$$

Expression (10) is the defining property of a *force-free, field-aligned current.*

We again emphasize that expression (2) implies that the existence of a non-zero valued $\boldsymbol{j}$ will produce a curl($\boldsymbol{B}$) vector at that point. If there is no $\boldsymbol{j}$ present, (10) is automatically fulfilled even if $\boldsymbol{B}$ is non-zero. This demonstrates that knowledge of the direction and magnitude of $\boldsymbol{B}$ at any given point generally yields no information about the magnitude, direction or even the existence of $\boldsymbol{j}$ at that point. However, knowledge of the direction and magnitude of the $\nabla \times \boldsymbol{B}$ vector at any given point *does* determine the value of μ $\boldsymbol{j}$ there. *Field-aligned, force-free currents* [Peratt [4], pp. 43-45] represent the lowest state of stored magnetic energy attainable in a cosmic current. We seek an expression for the magnetic field, $\boldsymbol{B}(r,\theta,z)$, in such a current/field structure.

III. Mathematical Model of a Field-Aligned Force-Free Current

Equation (10) can be expanded into differential equation form using the cylindrical coordinate definition of curl and the three-dimensional vector product determinant. This leads to an expression of complexity and little usefulness. But, because expression (10) is satisfied if and only if the current density, $\boldsymbol{j}$, has the same direction (except for sign) as $\boldsymbol{B}$ (although not necessarily having the same magnitude), it was suggested [Peratt, *op sit*] that

$$\left(\nabla \times \boldsymbol{B}\right) = \alpha \boldsymbol{B} \tag{11}$$

where α is any scalar, satisfies the requirement of (10) and avoids the complexity of its direct solution.

The properties and effects of α on the solution of (11) and interpretation of any results obtained thereby must be carefully delineated. The purpose of introducing the parameter α is for none other than to obey the requirement that the vector curl($\boldsymbol{B}$) and the vector $\boldsymbol{B}$ have the same direction as required in (10). The specific numerical value chosen for α in (11) is of no significance in any real-world electromagnetic processes. Alpha's only purpose is to facilitate a mathematical solution that yields functional forms for the components of $\boldsymbol{B}$. And that value is completely defined by the analyst who solves the equation. It is not necessary or even proper to be concerned about whether α's numerical value might change as a function of position, because it is completely controlled by whoever is solving (11). Its only valid property of interest is that it is an entity that contributes *zero angle* everywhere. Therefore, it must be recognized that the parameter α is not a physical quantity. It does not appear in expressions (1) through (10) that describe the basic, fundamental physical EM inter-relationships among the real physical entities. It cannot affect the values or relationship of $\boldsymbol{B}$ or $\boldsymbol{j}$ in the real world. All it does is to serve as a quantity that has no effect on the direction of the variable it multiplies. However, at this point, it is not clear whether or not a physically realizable solution of (11) for such a $\boldsymbol{B}$ field exists.

Since we are considering a Birkeland current, a convenient choice of coordinate system is the cylindrical system in which a point, $\boldsymbol{p}$, is represented by (r,θ,z), as illustrated in Fig 1.

The left side of expression (11) can be expanded in cylindrical coordinates as follows:

$$\nabla \times \boldsymbol{B} = \left(\frac{1}{r}\frac{\partial B_z}{\partial \theta} - \frac{\partial B_\theta}{\partial z},\ \frac{\partial B_r}{\partial z} - \frac{\partial B_z}{\partial r},\ \frac{1}{r}\frac{\partial}{\partial r}\left(rB_\theta\right) - \frac{1}{r}\frac{\partial B_r}{\partial \theta}\right) \tag{12}$$

And the right side of (11) can be expressed as

$$\alpha \boldsymbol{B} = \left(\alpha B_r,\ \alpha B_\theta,\ \alpha B_z\right) \tag{13}$$

In (12) and (13), all field components are functions of the position vector, ***p***. Equation (12) is simply the definition of the curl of ***B*** in cylindrical coordinates[10]. Given that there is assumed to be no variation of current density ***j*** in the θ and z directions, (2) and (4) imply the same is true for ***B***.

It follows from the absence of any externally applied forces (other than possibly a static axial electric field to maintain ***I***) and any time-varying electric fields, that all partial derivatives of ***B*** w.r.t. θ and z are zero and, therefore, what remains of (11) after these simplifications in (12) are the following three equations:

In the radial direction,

$$\alpha B_r = 0 \tag{14}$$

There is no radial component of the ***B*** vector (which is consistent with Maxwell's $\nabla \bullet \boldsymbol{B} = 0$).

In the azimuthal direction,

$$\frac{\partial B_z}{\partial r} = -\alpha B_\theta \tag{15}$$

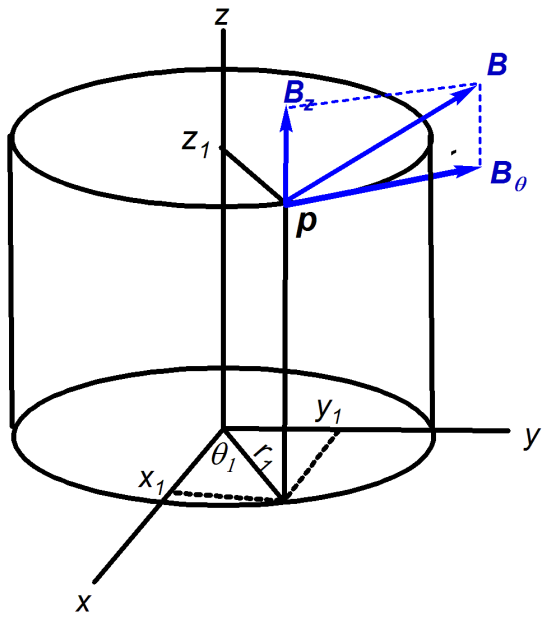

Fig. 1. Total magnetic field vector $\mathbf{B}\,(r_1, \theta_1, z_1) = \mathbf{B}$, and its two components $\mathbf{B}_z$ and $\mathbf{B}_\theta$ at a particular location (r_1, θ_1, z_1) ; $\mathbf{B}_r = 0$.

and in the axial direction,

$$\frac{1}{r}\frac{\partial}{\partial r}\left(r B_\theta\right) = \alpha B_z . \tag{16}$$

Thus, the essential result is two coupled differential equations (DEs) in the two dependent variables B_θ and B_z, as shown in expressions (15) and (16). The independent variable in both is radial distance, r.

IV. Solution in Closed Form

Combining expressions (15) and (16) yields a single second-order DE in a single dependent variable.

$$r^2 \frac{d^2 B_z(r)}{dr^2} + r\frac{d B_z(r)}{dr} + \alpha^2 r^2 B_z(r) = 0 \tag{17}$$

The single dependent variable $B_z(r)$ is the axial component of the force-free steady-state magnetic field. Following the Principle of Parsimony, no boundary condition at any non-zero value of r is introduced. The field $B_z(r)$ is allowed to extend as far as the DE (17) provides for. There will be, in all currents in space, a natural limit to the size of the plasma and therefore to the extent of the current density ***j***(r).

Continuing the earlier dimensional analysis of (4) – (7) we write, using (11), repeated here for reference:

$$\begin{aligned} &\left(\nabla \times \boldsymbol{B}\right) = \alpha \boldsymbol{B} \\ &\frac{Webers}{m^3} = \alpha \frac{Webers}{m^2} \\ &\frac{1}{m} = \alpha \end{aligned} \tag{18}$$

This indicates that α is functionally a distance scale factor that will vary the scale of the r-axis of the resulting plot of $B_z(r)$ in the mathematical model we are attempting to formulate.

Having now fully specified the DE (17), it is recognized as being identical to Bessel's equation of order zero, with scale parameter α (the units of which are the reciprocal of the units of r).

Recognizing (17), we have a closed-form solution for the dependent variable in that DE that results from expanding equation (11). The solution to Bessel's equation with scale factor α = unity is[11]

$$y = AJ_0(x) + CY_0(x) \tag{19}$$

where A and C are arbitrary constants. $J_0(x)$ is the Bessel function of the first kind and zeroth order, and $Y_0(x)$ is the Bessel function of the second kind (or sometimes called the Weber or Neumann function) of zeroth order. Similarly in

(17) with an arbitrary valued scale factor α, we find

$$y = AJ_0(\alpha x) + CY_0(\alpha x). \tag{20}$$

where

$$\begin{aligned} J_0(x) &= 1 - \frac{x^2}{2^2} + \frac{x^4}{2^2 4^2} - \frac{x^6}{2^2 4^2 6^2} + \ldots \\ &= 1 - \frac{(x/2)^2}{(1!)^2} + \frac{(x/2)^4}{(2!)^2} - \frac{(x/2)^6}{(3!)^2} + \ldots \end{aligned} \tag{21}$$

The function $J_0(\alpha x)$ has the value unity at the boundary $x = 0$, and the function $Y_0(\alpha x)$ has a singularity at this same boundary. Because reality dictates that the magnetic field be finite-valued, the value of arbitrary coefficient C must be set equal to zero. Thus, the solution to (17) is given specifically by

$$B_z(r) = B_z(0)J_0(\alpha r) \tag{22}$$

This can also be expressed in various other closed forms, but these are not needed here. This Bessel function of the first kind and of order zero can be used to produce Bessel functions of the first kind and orders 1, 2, 3, … simply by differentiating (21) term by term[11]. The recursion relation for the first order Bessel function is

$$J_1(x) = -\frac{dJ_0(x)}{dx}. \tag{23}$$

$$J_1(x) = \frac{x}{2} - \frac{x^3}{2^2 4} + \frac{x^5}{2^2 4^2 6} - \ldots \tag{24}$$

From expressions (15), (22), and (23), we obtain

$$B_\theta(r) = B_z(0)J_1(\alpha r) \tag{25}$$

Consequently, from (22) and (25), the scale of the spatial extent of the magnetic field in the radial direction is determined by α.

The Bessel functions can also be expressed in integral form as follows[7]:

$$J_0(x) = \frac{1}{\pi}\int_0^\pi \cos(x\sin\varphi)d\phi \tag{26}$$

$$J_1(x) = \frac{1}{\pi}\int_0^\pi \cos(x\sin\varphi - \varphi)d\varphi \tag{27}$$

These Bessel functions are sometimes called cylinder functions or cylindrical harmonics. They approach damped trigonometric functions for large r, but the amplitude decrease is very gradual – varying inversely as the *square root* of αr, which is a more gradual decay than the typical exponential, or $1/(\alpha r)$, or $1/(\alpha r)^2$ damping. This decay behavior can be seen from the asymptotic forms

$$\begin{aligned} J_0(x) &= \sqrt{\frac{2}{\pi x}}\left[\cos\left(x - \frac{\pi}{4}\right) + O\left(\frac{1}{x}\right)\right] \\ J_1(x) &= \sqrt{\frac{2}{\pi x}}\left[\cos\left(x - \frac{3\pi}{4}\right) + O\left(\frac{1}{x}\right)\right] \end{aligned} \tag{28}$$

Therefore, expressions (14), (22), and (25) for $B_r(r)$, $B_z(r)$ and $B_\theta(r)$ together provide a complete description of the magnetic field that surrounds and pervades the final force-free, minimum-energy, steady-state, cosmic current. In this state, all Lorentz forces have been reduced to zero. The physical implications of these expressions are fully described in section VII, below.

V. Euler Method of Solution

Another approach to solving (17) that does not require that it be recognized as a Bessel equation is to use an iterative numerical method. A major reason for performing such an analysis is that such numerical methods result in a plot of the dependent variable which reveals the effect of the parameter, α on the solution. One such method is based on a *state-variable representation* of the DE – in this case (17) or, equivalently, the pair (15) and (16). In order to describe expressions (15) and (16) in state-variable form, the product rule for derivatives is first applied to (16) as follows:

$$\frac{\partial(rB_\theta)}{\partial r} = r\alpha B_z \tag{29}$$

$$r\frac{\partial B_\theta}{\partial r} + B_\theta = r\alpha B_z. \tag{30}$$

Two state-variables may be defined as follows:

$$x_1 = B_z \tag{31}$$

$$x_2 = B_\theta \tag{32}$$

so that rewriting expressions (15) and (30) in state-variable form yields

$$\frac{dx_1}{dr} = -\alpha x_2 \tag{33}$$

and

$$\frac{dx_2}{dr} = \alpha x_1 - (1/r)x_2. \tag{34}$$

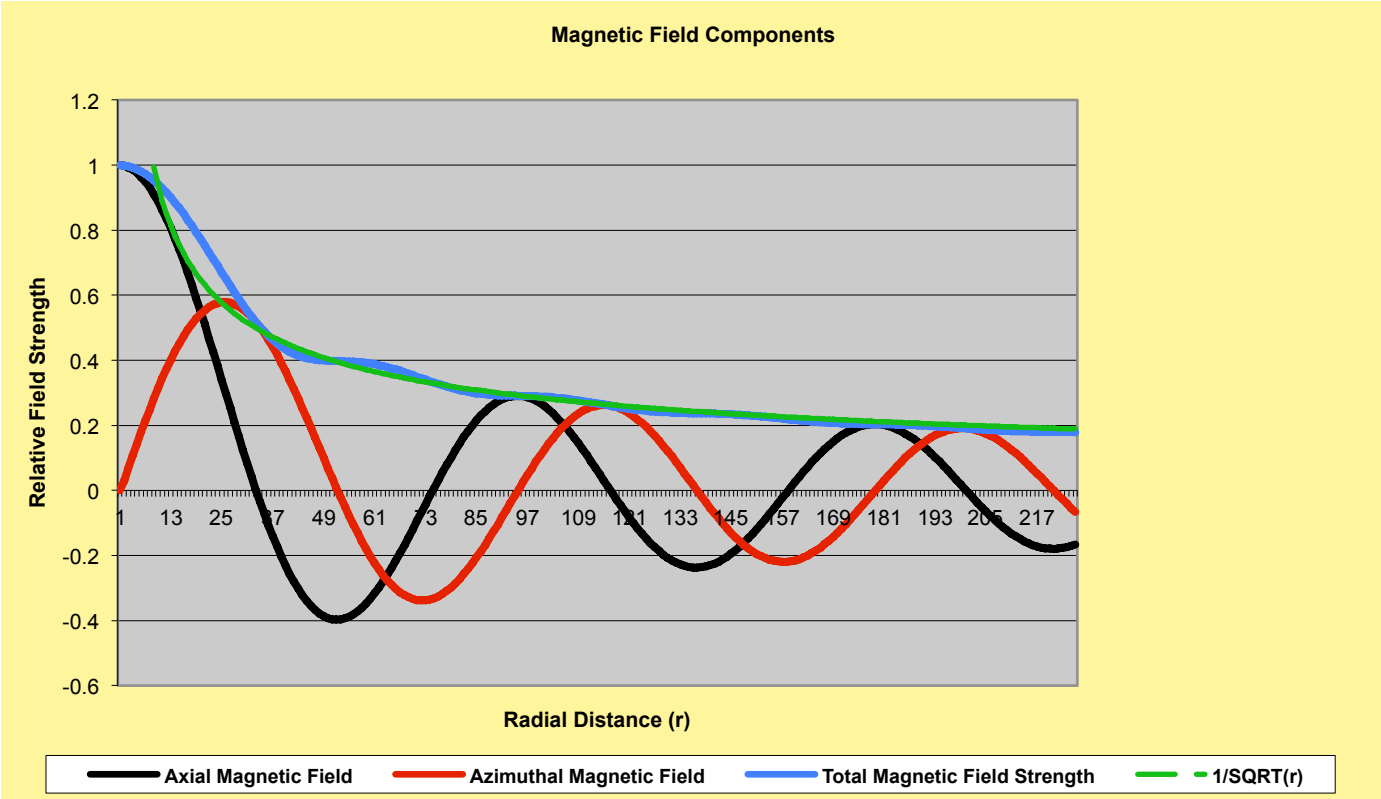

Fig. 2. Axial Magnetic Field component B_z , the Azimuthal Magnetic Field component B_θ, the magnitude of the Total Magnetic Field; and, for reference, a plot of 1/SQRT(r) – all vs. radial distance quantized to integer multiples of the step-size h = 0.1. The value of α used in (33) and (34) to achieve adequate resolution of the Bessel functions with this step-size is 0.075. The horizontal axis in this plot is the radius ***r***-axis. Note in Table I that in every case (row) the natural dimensionless Bessel function argument, $x = \alpha r$, thus demonstrating the scale factor utility of α. (e.g., 2.4048 = 0.075 x 33.)

Since there is only one independent variable, r , in these equations, the partial derivatives are replaced with full derivatives. This pair of equations is easily re-expressed as a first-order vector DE, with vector dimension two.

The Euler algorithm for obtaining an approximate step-wise solution to (33) and (34) was implemented. A spreadsheet was used to implement this iterative solution. In order to obtain good accuracy, a fourth-order Runge-Kutta predictor-corrector algorithm[12] was also incorporated. The results, presented in Fig. 2 show, as expected,: $B_z(r)$ the axial component, $B_\theta(r)$ the azimuthal component as well as the total magnetic field strength $|\boldsymbol{B}|$ (the square root of the sum of the squares of the two component fields, B_z and B_θ). The total field strength is strongest at a minimum radial value r and decreases with increasing r . The importance of performing this iterative solution lies in the fact that the parameter α is clearly shown to be a scale factor on the radius, r, variable. The value for that distance-scaling parameter was arbitrarily chosen to be $\alpha = 0.075$, and the Euler step increment was chosen to produce sufficient resolution at h = 0.1. The horizontal axis of Fig. 2 demonstrates the relationship between the non-dimensional argument of the Bessel functions, x, and the scaled variable, $\alpha\boldsymbol{r}$. Nothing what so ever is inferred or implied about the current density vector field, $\boldsymbol{j}$ at this stage.

The overall *Total Magnetic Field Magnitude* that is associated with a force-free, field aligned current decreases with increasing radial distance from the central axis of the current as $(\alpha r)^{-\frac{1}{2}}$ which is shown, for reference, in the fourth series plotted in Fig. 2. This result was fully described in section IV (see expression 28). Therefore, the magnetic fields within field-aligned cosmic currents extend outward in space much farther and less diminished in strength than the field that would be generated by a simple straight-wire electric current.

VI. Current Density of a Field-Aligned Current

The fundamental curl($\boldsymbol{B}$) Maxwell equation (repeated below) is valid at every point in the entire plasma

$$\nabla \times \boldsymbol{B} = \mu \boldsymbol{j} \tag{2}$$

This implies that wherever $\boldsymbol{j}$ is non-zero valued, it creates a collinear curl($\boldsymbol{B}$) vector at that point.

In section IV, the magnetic field of a fully relaxed force-free Birkeland current was determined in (14), (22), and (25), the last two repeated here as (35) and (36).

$$B_z(r) = B_z(0) J_0(\alpha r) \tag{35}$$

$$B_\theta(r) = B_z(0) J_1(\alpha r) \tag{36}$$

We now use these non-zero components of the ***B***-field to first determine the vector curl(***B***) at every point, and then to determine the corresponding current densities, $j_z(r)$ and $j_\theta(r)$. By definition the curl(***B***) is:

$$\nabla \times \boldsymbol{B} = \left(\frac{1}{r}\frac{\partial B_z}{\partial \theta} - \frac{\partial B_\theta}{\partial z},\ \frac{\partial B_r}{\partial z} - \frac{\partial B_z}{\partial r},\ \frac{1}{r}\frac{\partial}{\partial r}(rB_\theta) - \frac{1}{r}\frac{\partial B_r}{\partial \theta} \right) \tag{37}$$

Now, using (14), we have:

in the *r* direction: $0 = \mu j_r$ (38)

This confirms an initial assumption.

In the θ direction: $-\frac{\partial B_z}{\partial r} = \mu j_\theta$ (39)

In the *z* direction: $\frac{1}{r}\frac{\partial}{\partial r}(rB_\theta) = \mu j_z$ (40)

Inserting (35) and (36) into (39), and (40) yields

From (39) $$-\frac{\partial}{\partial r}\left[B_z(0) J_0(\alpha r)\right] = \mu j_\theta \tag{41}$$

$$B_z(0) J_1(\alpha r) = \mu j_\theta \tag{42}$$

From (40) $$\frac{1}{r}\left[r\frac{\partial B_\theta}{\partial r} + B_\theta \right] = \mu j_z \tag{43}$$

$$\frac{\partial B_\theta}{dr} + \frac{1}{r} B_\theta = \mu j_z \tag{44}$$

$$B_z(0)\left[\frac{\partial J_1(\alpha r)}{\partial r} + \frac{1}{\alpha r} J_1(\alpha r) \right] = \mu j_z \tag{45}$$

Since

$$\frac{\partial J_1}{\partial x} = J_0 - \frac{1}{x} J_1 \tag{46}$$

Then (45) becomes

$$B_z(0)\left[J_0(\alpha r) - \frac{1}{\alpha r} J_1(\alpha r) + \frac{1}{\alpha r} J_1(\alpha r) \right] = \mu j_z \tag{47}$$

So

$$B_z(0) J_0(\alpha r) = \mu j_z \tag{48}$$

Therefore from (42) and (48), the magnitude of both $j_z(r)$ and $j_\theta(r)$ depend ***only*** on the values of $B_z(0)$ and μ. The radial scale depends on α.

VII. Consequences of the Oscillatory Nature of the Solution

The expressions for the current-density and magnetic-density distributions within a steady-state, force-free, field-aligned Birkeland current are re-listed, together, here:

$$B_z(r) = B_z(0) J_0(\alpha r) \tag{22}$$

$$B_\theta(r) = B_z(0) J_1(\alpha r) \tag{25}$$

$$j_z(r) = \frac{B_z(0)}{\mu} J_0(\alpha r) \tag{48}$$

$$j_\theta(r) = \frac{B_z(0)}{\mu} J_1(\alpha r) \tag{42}$$

This then is the structure of a minimum (Lorentz force) energy, field-aligned current. Taken together these four expressions imply several properties of these current density / magnetic field vectors:

1. There are no points within the plasma where ***j*** = 0 or ***B*** = 0. A non-zero, finite current density and a non-zero magnetic field exist at every point. In the first paragraph after expression (1) it was stated, "Nor are any assumptions made about the distribution of the current density across the cross-section." Expressions (42) and (48) have derived this property. We have not assumed this property.
2. At every such point ***j*** and ***B*** are collinear.
3. At every such point $\mu\boldsymbol{j} = \boldsymbol{B}$. So μ is the only proportionality constant relating j and ***B***.

The model (these four expressions) remains valid only over the range $0 < r < R$. Farther out from the *z*-axis than $r = R$, $j = 0$. From that point outward, the cylindrical plasma looks more and more like a single straight, current-carrying wire. So beyond that point, the magnetic field strength will decay approaching $1/r$. This is clearly demonstrated by inserting $\alpha = 0$ and $B_\theta = k/r$ into (30) which satisfies that equation.

This force-free current structure is in stable equilibrium (as is any minimum energy system). Visualizing this field structure with the aid of Figs. 2, 3, and 5, reveals that, within the plasma, at increasing radial values, the magnetic field, together with its corresponding current density, wrap around the axis of the current stream with a continuously varying helical pitch angle. There is no non-zero B_r component anywhere. Therefore the ***j*** vector at every point in the Birkeland current is aligned with its corresponding ***B*** vector. As a result this affords a mechanism for maintaining the stability of the structure.

For example[13], in this cylindrical geometry, the magnetic field, ***B***, as well as the current field, ***j*** generally

follow spiral paths (straight lines on any θ-z plane). If we change the Lorentz angle between them, say, by temporarily increasing the total current, $\boldsymbol{I}$, making the $\boldsymbol{j}$

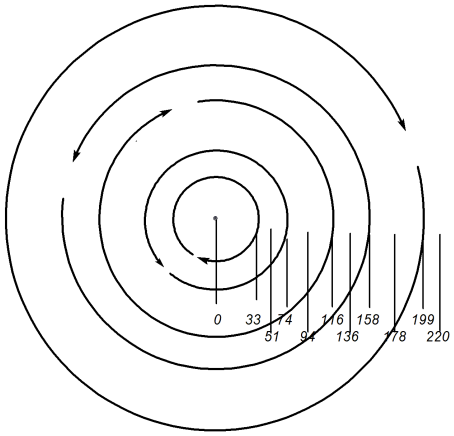

Fig. 3. Cross-section view of a force-free current and the directions of its associated magnetic field. In this view the reader is looking in the +z-direction (in the direction of main current flow). The radius values shown are quantized to integer multiples of x (h = 0. 1, with α = 0.075), which were used in the Euler iterative solution of (33)

direction more axial than the $\boldsymbol{B}$ vector, a Lorentz force will push inward counteracting any expansion.

The two methods of solution described in Sections IV and V (the closed form Bessel functions in expressions (22) – (25) and the Euler-RK numerical approximation illustrated in Fig. 2) are, essentially, the same solution.

Both solutions demonstrate repeated reversals in the directions of both the axial and the azimuthal magnetic field components with increasing radial distance. This implies (1) the existence of a discrete set of virtual concentric cylindrical surfaces, centered on the axis of the field-aligned current, at which the axial field component, B_z is zero-valued and the azimuthal magnetic component, B_θ, is alternatingly CW and CCW. The axial and azimuthal field strengths are seen to be in quadrature. For example in Fig. 2, in a region such as that between radial distances 74 and 116, the axial field, B_z, is unidirectional (in the positive z-direction, attaining maximum strength at $r \cong 94$); whereas the azimuthal field reverses direction at $r \cong 94$, changing from the negative direction of θ to the positive direction. This results in a total magnetic field vector that wraps the current stream, its pitch angle rotating (with increasing r) in a clockwise direction when viewed inward along a radius, toward the central axis of the current (see Fig. 5).

Thus, the axis of a cosmic, field-aligned current is seen to be wrapped with a compound helical magnetic field whose angle wrt the +z-axis increases continuously with increasing radial distance. This gives rise to a structure suggestive of some ancient Roman fasces. Fasces are made by putting together a bundle of thin, fragile reeds or sticks that, taken separately, can be easily broken. The bundle is then wrapped tightly together along its entire length by spiraling leather straps. In final form the finished fasces is extremely strong and cannot be easily bent or broken.

It is noted that the Alfvén image[14] shown in Fig. 6, which is often used to describe the Birkeland current steady-state minimum-energy magnetic field, is in agreement with these results, but it only describes the actual morphology for small r. As r increases beyond what is shown in Fig. 6, a continued rotation of the pitch angle of the magnetic/current helixes occurs. This rotation does not abruptly stop at 90° (where the total magnetic field is orthogonal to the direction of z) as might be inferred from Fig. 6. The helical (fasces-like) wrapping continues with increasing radius values and strengthens the field-aligned current structure.

The qualitative properties of the plots in Fig. 2 and their implications are listed in Table I.

TABLE I

IMPORTANT RADIUS VALUES FOR MAGNETIC COMPONENTS			
Radius Values $r = x/\alpha$	Zeros of $J_0(x)$ X	Zeros of $J_1(x)$ x	Description
0		0	B_z pos max, B_θ zero.
33	2.4048		B_z zero, B_θ pos max
51		3.8317	B_z neg max, B_θ zero
74	5.5201		B_z zero, B_θ neg max
94		7.0156	B_z pos max, B_θ zero
116	8.6537		B_z zero, B_θ pos max
136		10.1735	B_z neg max, B_θ zero.
158	11.7915		B_z zero, B_θ neg max
178		13.3237	B_z pos max, B_θ zero
199	14.9309		B_z zero, B_θ pos max

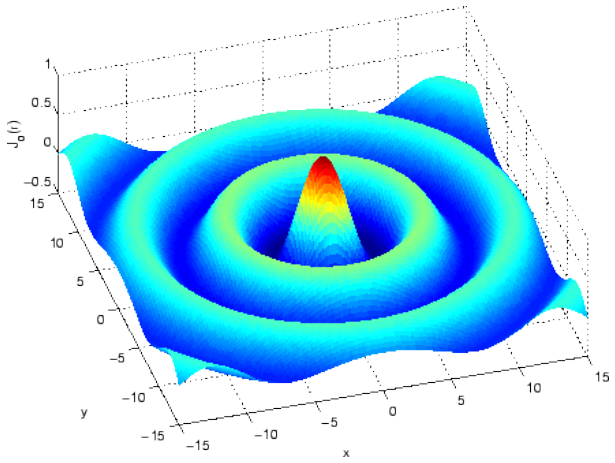

Fig. 4. Three-dimensional plot of the magnitude of the axial magnetic field component, $B_z(r)$. This demonstrates the relative strength of the central (on-axis) magnetic field. It does not include the effects of the azimuthal (wrap-around) magnetic field component, B_θ.

VIII. Validity Check on Solutions

One question still remains regarding the validity of these solutions: expressions (14), (22), (25), (38), (42) and (48) for $B_r(r)$, $B_\theta(r)$, $B_z(r)$, $j_r(r)$, $j_\theta(r)$, and $j_z(r)$. Directly or indirectly all six of these quantities result from solving the

Bessel equation (17), which, itself, is directly derived from Peratt's substitute equation (11), not from the fundamental, defining expression of a *force-free current* (10). This

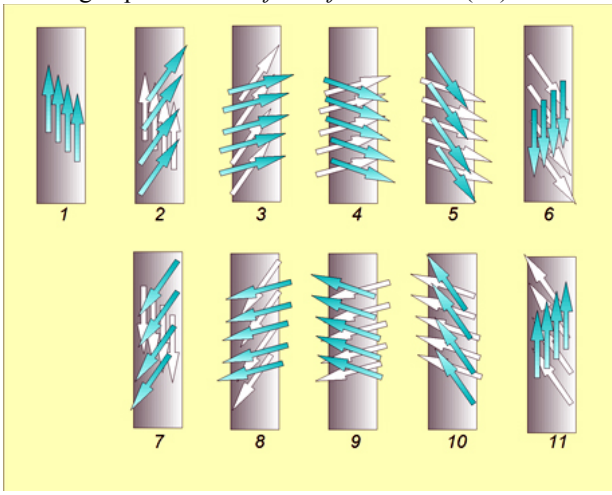

Fig. 5. Pitch angle of the helical vector-valued total magnetic field, ***B***, that encircles a field-aligned current changes continuously with increasing radial distance from the central axis of the current. There are no quantum jumps in this angle or in the field's magnitude. In this figure, one cycle (0°-360°) of the pitch angle is shown. The cycle is sketched at eleven increasing sample values of radius. The shaded arrows show the total magnetic field direction at each value of radius, *r*, and the white arrows show the field direction at an increment just below each of those values of radius. At every point the current density, ***j*** is collinear with ***B***.

substitute, (11), was posited as being a workable alternative to (10), the defining property. Expressions (10) and (11) impose *similar* but not identical requirements on the magnetic field $\boldsymbol{B}(r,\theta,z)$ and the current density field $\boldsymbol{j}(r,\theta,z)$. Expression (10) imposes only the simple requirement that ***B*** and ***j*** are collinear. Expression (11) requires not only that they be collinear but that they have some fixed numerical proportionality defined as α. It has not yet been demonstrated that the vector field solutions of (11) listed in the first line of this section are actually valid solutions of the fundamental, defining expression (10).

In order to prove (14), (22), and (25) are solutions of (10) we insert those solutions back into (10). We write the central three dimensional cross-product contained in expression (10) in determinant form.

$$(\nabla\times\boldsymbol{B})\times\boldsymbol{B}=\begin{vmatrix}\hat{\boldsymbol{r}} & \hat{\boldsymbol{\theta}} & \hat{\boldsymbol{z}}\\ (\nabla\times\boldsymbol{B})_r & (\nabla\times\boldsymbol{B})_\theta & (\nabla\times\boldsymbol{B})_z\\ \boldsymbol{B}_r & \boldsymbol{B}_\theta & \boldsymbol{B}_z\end{vmatrix} \tag{49}$$

Using the cylindrical curl expansion of (12)

$$(\nabla\times\boldsymbol{B})\times\boldsymbol{B}=\begin{vmatrix}\hat{\boldsymbol{r}} & \hat{\boldsymbol{\theta}} & \hat{\boldsymbol{z}}\\ 0 & -\dfrac{\partial B_z}{\partial r} & \dfrac{1}{r}\dfrac{\partial}{\partial r}(rB_\theta)\\ B_r & B_\theta & B_z\end{vmatrix} \tag{50}$$

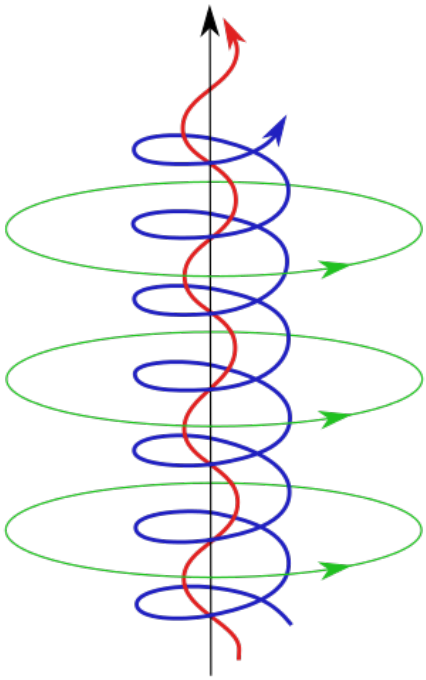

Fig. 6. Alfvén image showing the helical angle of the colinear ***j*** and ***B*** vectors as a function of radius, *r*. [14]

We use $B_r(r)=0$, (22) and (25).

So in (50) the [22] element becomes as in (41)

$$-\frac{\partial}{\partial r}\left[B_z(0)J_0(\alpha r)\right]=B_z(0)J_1(\alpha r) \tag{51}$$

The [23] element becomes

$$\frac{1}{r}\left(r\frac{\partial B_\theta}{\partial r}+B_\theta\right)=\frac{\partial B_\theta}{\partial r}+\frac{1}{r}B_\theta \tag{52}$$

$$B_z(0)\left[\frac{\partial J_1(\alpha r)}{\partial r}+\frac{1}{\alpha r}J_1(\alpha r)\right]. \tag{53}$$

Since

$$\frac{\partial J_1}{\partial x}=J_0-\frac{1}{x}J_1, \tag{54}$$

then (53) becomes

$$B_z(0)\left[J_0(\alpha r)-\frac{1}{\alpha r}J_1(\alpha r)+\frac{1}{\alpha r}J_1(\alpha r)\right] \quad (55)$$

$$B_z(0)\left[J_0(\alpha r)\right] \quad (56)$$

Using (51), (56), (14), (22), and (25) in (50) and omitting functions' arguments for simplicity

$$(\nabla\times\boldsymbol{B})\times\boldsymbol{B}=\begin{vmatrix}\hat{\boldsymbol{r}} & \hat{\boldsymbol{\theta}} & \hat{\boldsymbol{z}}\\ 0 & B_0J_1 & B_0J_0\\ 0 & B_0J_1 & B_0J_0\end{vmatrix}=0 \quad \text{(QED)} \quad (57)$$

Note that (57) is valid independent of whatever value of scale factor α is included in the arguments of the Bessel functions. Thus, we conclude that $B_r(r)$=0, (22), and (25) are exact solutions of (10), the original defining DE of a *force-free, field-aligned* current. This result is valid whether or not the alternative DE (11) had ever been introduced. Whether or not the parameter α "varies with position" (or for any other reason) is a false concern. Expressions (18)-(20) make it clear that α is simply a scale factor of the radius, r, that makes it possible to model various sized cosmic currents. The original defining DE, expression (10), is satisfied by the Bessel function solution set presented in section VII: $\boldsymbol{B}(r,\theta,z)$, and $\boldsymbol{j}(r,\theta,z)$.

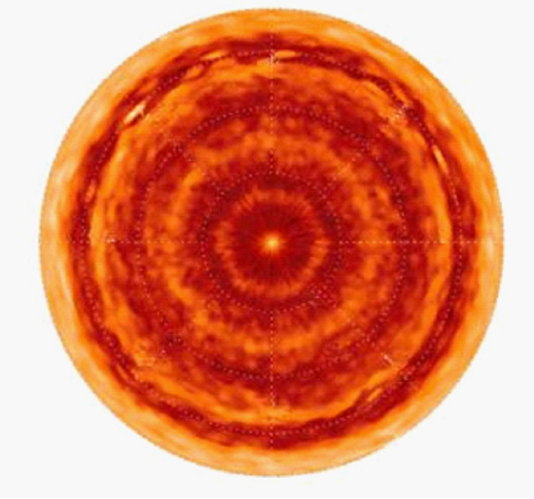

Fig. 7. North pole region of Saturn Infrared image.[15]
Image Credit: NASA/JPL/Oxford University

IX. Comparison of Results with Observations

1. Laboratory Results.

It is not known if any actual, observed cosmic currents are in the minimum (Lorentz force) energy, field-aligned state. Several apparently show evidence of near-force-free behavior.

The image shown in Fig. 8 was obtained in a plasma laboratory. Neither this nor the image of Saturn's north pole in Fig. 7 represent force-free currents because they both are images of collisions of such currents with material objects. Fig. 8 does suggest what may occur if an overall current increase were to occur. The force-free structure would begin to undergo changes (if not be totally destroyed). Exactly what would happen is pure conjecture but if one starts with Fig. 3 and considers what might happen if a low intensity stream of positive charge began to infuse the entire cross-section in a $+z$ direction (away from the reader), these additional positive charges would likely be deflected by Lorentz forces as follows:

At radii 33, 116, and 199 – deflection inward and CW.

At radii 74, and 158 – deflection outward and CCW.

The two paths (inward and CW at r = 116 and the one at r = 74 moving outward and CCW) might appear to be a single path spiraling inward from r = 116 toward r = 74. Such pathways are suggested in Fig. 8. Clearly in that state, the system is no longer at minimum energy – Lorentz forces are at work within the no-longer force-free plasma.

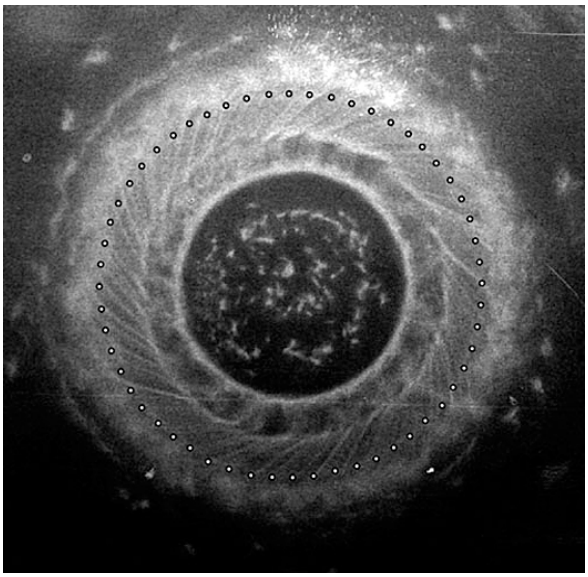

Fig. 8. Penumbra of a dense plasma focus discharge from a current of 174,000 A. Credit A. L. Peratt

In the steady-state minimum energy configuration, all Lorentz forces have been eliminated (submitted to) and charge simply follows the magnetic field structure. For example, positively charged matter, q_a, located at r = 158, has counter-clockwise motion. Any additional incoming $+z$-axial charges would be deflected outward, the combined motion describing an outward CCW path.

Similarly, charged matter, q_b, traveling clockwise at r = 199 would have additional incoming ($+z$ directed) charges that would end up traveling inward and CW. Plotting the paths of both q_a and q_b would likely look like a single diagonal (spiraling) pathway. See Fig. 8.

2. Astronomical Images.

Images presented in Figs. 7, 9, and 10 have been obtained from actual astronomical observations. It is well known that currents in plasma drag un-ionized (as well as ionized) matter along in their path. Fig. 3 implies that CW and CCW

counter-rotating current paths such as those at $r = 33$ and 74 ought to exhibit such counter-rotation. The image shown in Fig. 7 is consistent with the hypothesis that Saturn is receiving a flow of electric charge via a Birkeland current directed into its north pole much as Earth is known to be experiencing. This image was discussed by S. Smith in 2013 and by NASA[15].

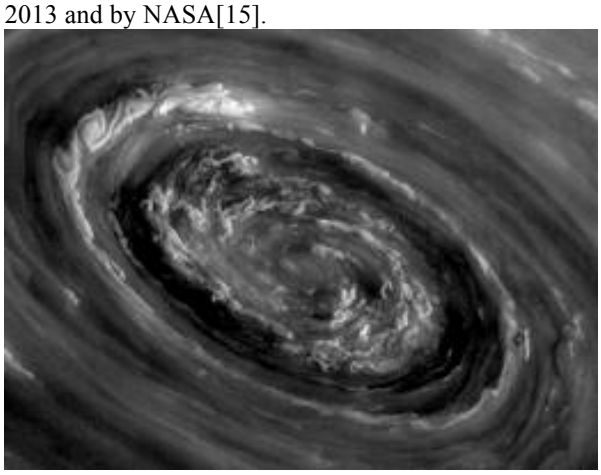

Fig. 9. Series of diocotron (shear) instabilities, especially obvious in the upper left of this image. This was taken from the NASA video which clearly shows counter-rotation.

For several years it was unknown, whether the circular paths appearing in Figs 7 and 8 are truly counter-rotating. It would require a video to reveal that kind of motion. It happens that NASA has produced exactly such a video showing counter-rotating (plasma) clouds within what appears to be the hexagonal shape at Saturn's north pole. See:

HTTP://SATURN.JPL.NASA.GOV/MULTIMEDIA/VIDEOS/MOVIES/CASSINI_SATURN_HURRICANE_480CC.MOV

In this video, the term "hurricane" is used repeatedly by the narrator who seems concerned about the fact that the 'storm' is fixed to the planet's north pole and that no water ocean exists below it to cause it to exist. He seems to be unconcerned that actual hurricane winds do not counter-rotate as these do. Matter that is even partially ionized can become radially stratified in a Birkeland current. Neutral dust can be carried along in the process. In the video, in shear regions between counter-rotating shells, what appear to be Diocotron instabilities can be seen (Fig. 9). Without NASA's video, the counter-rotational motions of these areas in the Saturnian surface would not be observed and therefore their existence would go undiscovered. This motion picture is crucial evidence of what is being presented here.

3. Circular Polarization in Gamma-Ray Bursts

In a Birkeland current both the current-density field and the aligned magnetic field associated with it rotate continuously with increasing radial distance, and this suggests itself as a leading candidate for explaining the newly discovered circular polarizations of afterglows from gamma-ray bursts and quasars. A recent paper in *Nature*[16] states,

> "Afterglow polarization directly probes the magnetic properties of the jet when measured minutes after the burst, and it probes the geometric properties of the jet and the ambient medium when measured hours to days after the burst. High values of optical polarization detected minutes after the burst of GRB 120308A indicate the presence of large-scale ordered magnetic fields originating from the central engine[a] (the power source of the GRB). Theoretical models predict low degrees of linear polarization and no circular polarization at late times, when the energy in the original ejecta is quickly transferred to the ambient medium and propagates farther into the medium as a blast wave. A possible explanation is to invoke anisotropic (rather than the commonly assumed isotropic) electron pitch-angle distributions, and we suggest that ***new models are required*** to produce the complex microphysics of realistic shocks in relativistic jets." [Emphasis added.]

X. CONCLUSIONS

The primary result of this paper is the discovery of the fact that the definition of what constitutes a force-free current-density-field/magnetic-field relationship 1) dictates that these two vector fields [$\boldsymbol{j}(r,\theta,z)$ and $\boldsymbol{B}(r,\theta,z)$] be everywhere aligned and 2) reveals that the overall solutions that specify the spatial dependence of those fields' strengths and directions are Bessel functions.

This leads, through straightforward mathematical analysis, to a number of important mathematical characterizations of these fields that are in strong agreement with reliable imagery obtained from both actual observations and measurements of phenomena in space and of plasma experiments in laboratories. The most salient conclusions drawn from this mathematical modeling and analysis are summarized here:

1. Magnetic fields produced by Birkeland currents stretch out radially from the central axis of the current stream much farther, and with greater potential effect, than previously thought. For large radial distances, r, the amplitudes of those helical fields decay slowly in inverse proportion to the square root of r as far as the extent of the plasma $r < R$.
2. The helical structure of these fields is richer than previously thought. For example, the angle of pitch of the helix varies smoothly and continuously with increasing radial distance from the central axis of the current out as far as the plasma current-carrying charges extend.
3. The stability of the fasces-like wrapping of the magnetic field explains the observed inherent stability of Birkeland currents over long interplanetary, inter-stellar, and inter-galactic distances. The Birkeland current 'jet' emanating from galaxy M 87 remains collimated over a distance exceeding 5000 light years[17].

It is hoped that this paper illustrates an important scientific principle that, if adhered to by the astrophysics community, will lead to better science in the pursuit of a deeper understanding of the workings of the Universe. This principle is nicely stated by the late Professor Ronald Newbold Bracewell[18], 1921-2007, pioneering radio astronomer, who said in the forward to a book written more than 25 years ago, which presents an innovative empirically-based mathematical theory for statistical analysis of data, as an alternative to the abstract stochastic process theory that is not derived from data, "…if we are to go beyond pure mathematical deduction and make advances in the realm of phenomena, theory should start from the data. To do otherwise risks failure to discover that which is not built into the model."

The conclusions drawn from the analysis of the observations-based mathematical model adopted in the present paper were tested against the original motivating observations and measurements, and consistently strong agreement was found. For example, the observed counter-rotating plasma (so called "winds") of Saturn's north polar region constitute strong supporting evidence for the presence there of the Birkeland current phenomenon studied in this paper, similar to what has been confirmed regarding the Birkeland current that powers the Earth's auroras. Many otherwise enigmatic images stand witness to the advisability of considering possible electrical causation of cosmic plasma phenomena. The M2-9 "Hourglass" planetary nebula is a prime case in point. It is suggested that the narrowing of the conducting channel due to the z-pinch transitions the plasma from the dark mode into the visible glow and arc modes.

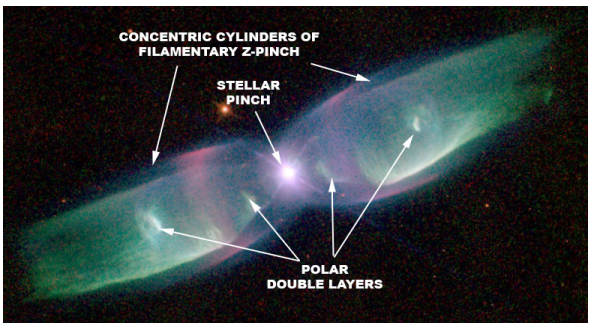

Fig. 10. The "Hourglass" planetary nebula, M2-9 showing at least two of the concentric surfaces that constitute the Birkeland current forming the object as well as plasma double layers that form in strong current discharges.

ACKNOWLEDGMENT

The author wishes to express his sincere thanks to Dr. Jeremy Dunning-Davies for recognizing that the differential equation derived in this study is a Bessel Equation, whose solutions are given by the Bessel functions, J_0 and J_1. He also gave the author encouragement and much needed advice.

Dr. William A. Gardner did extensive work regarding the closed form solution of the Bessel equation and provided advice and much of the supportive mathematical rigor included here. He has extensive knowledge of the logic of mathematics and engineering. Dr. Timothy Eastman of NASA's Goddard Space Center, Dr. Ron DeLyser, EE Department U. of Denver, and Dr. C.J. Ransom of Vemasat Labs gave freely and graciously of their time, advice, and assistance to help in this effort.

REFERENCES

[1] K. Birkeland, *The NorwegianPolaris Expedition 1902-1903*, Vol. 1, Sect. 1, Aschehoug, Oslo

[2] H. Alfvén, COSMIC PLASMA, (Book) Boston, D. Reidel, 1981 p.1.

[3] Mariner-Venus 1962 Final Project Report, NASA-SP59, Scientific and Technican Information Division, 1965, Washington, DC.

[4] A. L. Peratt, PHYSICS OF THE PLASMA UNIVERSE. (Book) Springer-Verlag, New York, 372 pages, 1992. p. 44.

[5] A. Dessler, Editor Geophysical Research Letters, A. L. Peratt, personal communication.

[6] C-G. Falthammer,: "Magnetosphere-ionosphere interaction–near-earth manifestations of the plasma universe," IEEE Tran. Plasma Sci. 14 616 (1986).

[7] T. Potemra, "Alfvén Waves and Birkeland Currents", Physica Scripta Vol. T60, 107-112, 1995, The Johns Hopkins University, Applied Physics Laboratory, Laurel, MD.

[8] J. Eastwood, Flux ropes, NASA, Goddard Space Flight Center, Greenbelt, MD., 2009.

[9] H. B. Callen, THERMODYNAMICS AND AN INTRODUCTION TO THERMOSTATISTICS (2nd Ed. ed.). New York: John Wiley

[10] Reference Data for Radio Engineers 4th edition (1956) ITT, New York, p. 1065, 1088.

[11] Matlab, Bessel functions of the First and Second Kind. http://www.mhtlab.uwaterloo.ca/courses/me755/web_chap4.pdf.

[12] Runge-Kutta Method, Wolfram MathWorld; http://mathworld.wolfram.com/Runge-KuttaMethod.html

[13] H. Alfvén, COSMIC PLASMA, (Book) Boston, D. Reidel, 1981 p.96 .

[14] H. Alfvén, "Evolution of the Solar System", Washington. D.C., USA: Scientific and Technical Information Office, National Aeronautics and Space Administration. (1976).

[15] NASA Cassini: Available: https://www.thunderbolts.info/wp/2012/11/28/saturns-northern-hot-spot/ and also http://saturn.jpl.nasa.gov/news/newsreleases/newsrelease20130429/

[16] K. Wiersema, et.al. "Circular polarization in the optical afterglow of GRB 121024A", Nature, 509, pages 201–204 (08 May 2014).

[17] H. Marshall, MIT, *M87's Energetic Jet*, APOD Dec 11 2004 http://apod.nasa.gov/apod/ap041211.html.

[18] W. A. Gardner. STATISTICAL SPECTRAL ANALYSIS: A NONPROBABILISTIC THEORY. (Book) Prentice-Hall, Englewood Cliffs, NJ, 565 pages, 1987. AUTHOR'S COMMENTS. SIAM Review, Vol. 36, No. 3, pp. 528-530, 1994.